

High-performance InAlGaN/GaN enhancement-mode MOS-HEMTs grown by pulsed metal organic chemical vapor deposition

Ya-Chao Zhang(张雅超), Zhi-Zhe Wang(王之哲), Rui Guo(郭蕊), Ge Liu(刘鸽),Wei-Min Bao(包为民), Jin-Cheng Zhang(张进成), and Yue Hao(郝跃)

Citation: Chin. Phys. B . 2019, 28(1): 018102. **doi:** 10.1088/1674-1056/28/1/018102
Journal homepage: http://cpb.iphy.ac.cn; http://iopscience.iop.org/cpb

What follows is a list of articles you may be interested in

Characteristics and threshold voltage model of GaN-based FinFET with recessed gate

Chong Wang(王冲), Xin Wang(王鑫), Xue-Feng Zheng(郑雪峰), Yun Wang(王允), Yun-Long He(何云龙), Ye Tian(田野), Qing He(何晴), Ji Wu(吴忌), Wei Mao(毛维), Xiao-Hua Ma(马晓华), Jin-Cheng Zhang(张进成), Yue Hao(郝跃)
Chin. Phys. B . 2018, 27(9): 097308. **doi:** 10.1088/1674-1056/27/9/097308

Groove-type channel enhancement-mode AlGaN/GaN MIS HEMT with combined polar and nonpolar AlGaN/GaN heterostructures

Xiao-Ling Duan(段小玲), Jin-Cheng Zhang(张进成), Ming Xiao(肖明), Yi Zhao(赵一), Jing Ning(宁静), Yue Hao(郝跃)
Chin. Phys. B . 2016, 25(8): 087304. **doi:** 10.1088/1674-1056/25/8/087304

An analytical model for nanowire junctionless SOI FinFETs with considering three-dimensional coupling effect

Fan-Yu Liu(刘凡宇), Heng-Zhu Liu(刘衡竹), Bi-Wei Liu(刘必慰), Yu-Feng Guo(郭宇峰)
Chin. Phys. B . 2016, 25(4): 047305. **doi:** 10.1088/1674-1056/25/4/047305

Influences of fringing capacitance on threshold voltage and subthreshold swing of a GeOI metal-oxide-semiconductor field-effect transistor

Fan Min-Min, Xu Jing-Ping, Liu Lu, Bai Yu-Rong, Huang Yong
Chin. Phys. B . 2015, 24(3): 037303. **doi:** 10.1088/1674-1056/24/3/037303

Non-recessed-gate quasi-E-mode double heterojunction AlGaN/GaN high electron mobility transistor with high breakdown voltage

Mi Min-Han, Zhang Kai, Chen Xing, Zhao Sheng-Lei, Wang Chong, Zhang Jin-Cheng, Ma Xiao-Hua, Hao Yue
Chin. Phys. B . 2014, 23(7): 077304. **doi:** 10.1088/1674-1056/23/7/077304

High-performance InAlGaN/GaN enhancement-mode MOS-HEMTs grown by pulsed metal organic chemical vapor deposition*

Ya-Chao Zhang(张雅超)[1,†], Zhi-Zhe Wang(王之哲)[2], Rui Guo(郭蕊)[1], Ge Liu(刘鸽)[1], Wei-Min Bao(包为民)[3], Jin-Cheng Zhang(张进成)[1], and Yue Hao(郝跃)[1]

[1] *State Key Discipline Laboratory of Wide Band Gap Semiconductor Technology, School of Microelectronics, Xidian University, Xi'an* 710071, *China*
[2] *China Electronic Product Reliability and Environmental Testing Research Institute, Guangzhou* 510610, *China*
[3] *School of Aerospace Science and Technology, Xidian University, Xi'an* 710071, *China*

(Received 25 August 2018; revised manuscript received 22 October 2018; published online 12 December 2018)

Pulsed metal organic chemical vapor deposition was employed to grow nearly polarization matched InAlGaN/GaN heterostructures. A relatively low sheet carrier density of 1.8×10^{12} cm^{-2}, together with a high electron mobility of 1229.5 cm^2/V·s, was obtained for the prepared heterostructures. The surface morphology of the heterostructures was also significantly improved, i.e., with a root mean square roughness of 0.29 nm in a 2 μm×2 μm scan area. In addition to the improved properties, the enhancement-mode metal–oxide–semiconductor high electron mobility transistors (MOS-HEMTs) processed on the heterostructures not only exhibited a high threshold voltage (V_{TH}) of 3.1 V, but also demonstrated a significantly enhanced drain output current density of 669 mA/mm. These values probably represent the largest values obtained from the InAlGaN based enhancement-mode devices to the best of our knowledge. This study strongly indicates that the InAlGaN/GaN heterostructures grown by pulsed metal organic chemical vapor deposition could be promising for the applications of novel nitride-based electronic devices.

Keywords: InAlGaN, enhancement-mode, metal–oxide–semiconductor high electron mobility transistor, threshold voltage

PACS: 73.40.Kp, 81.05.Ea, 85.30.De **DOI:** 10.1088/1674-1056/28/1/018102

1. Introduce

Owing to the enormous potential in high power and high frequency applications, the GaN based high electron mobility transistors (HEMTs) have attracted tremendous attention in the past two decades.[1–3] One of the core issues in recent research is the realization and optimization of the enhancement-mode (E-mode) devices with positive threshold voltage (V_{TH}), which is crucial for the safe operation in the power electronic applications and various monolithic integrated digital circuits.[4] Various methods have been tested to achieve the E-mode HEMTs, which include the gate recess,[5,6] fluorine plasma ion implantation,[7–9] and P-type GaN gate.[10–12] However, all of these techniques require additional procedures during the device fabrication processes, which may adversely affect the technical repeatability and the device reliability.

Recently, the employment of quaternary InAlGaN/GaN heterostructure was proposed as a novel approach to fabricate the E-mode HEMTs, which only relies on the material growth techniques and is easy to control.[13–17] By adjusting the alloy composition, the InAlGaN barrier can be polarization matched with the GaN channel, and thus the sheet carriers in the channel are depleted at zero gate bias. Jena *et al.* have calculated the polarization matched conditions of the InAlGaN/GaN heterostructures, which show great design freedom of this system.[18] In addition, the previous reports revealed that the adoption of the InAlGaN barrier is beneficial to suppress the gate leakage and current collapse effects.[19] However, some challenges still exist in current research. On one hand, the InAlGaN barrier with low indium content may not accomplish the polarization matched condition with the GaN channel, and leads to V_{TH} of the devices lower than 1 V which cannot meet the requirement of 3 V or even higher for practical applications. On the other hand, the current output characteristics of the InAlGaN based E-mode devices with the saturation drain current density below 54 mA/mm are unsatisfactory.[13–17]

The main obstacle of the research lies in the difficulties in the growth of high quality InAlGaN material, as well as accurate control of the close polarization matched InAlGaN/GaN heterostructures. Recently, we proposed a pulsed metal organic chemical vapor deposition (MOCVD) growth technique for the epitaxy of InAlN and InGaN based heterostructures which possess excellent structural and transport properties.[20–25] Moreover, the thickness and alloy component of the epitaxial film can be accurately controlled in the pulsed MOCVD process. These results suggest that pulsed MOCVD could be a promising method to address the issues in the growth of high quality InAlGaN based heterostructures. In this work, the nearly polarization matched InAlGaN/GaN

*Project supported by the National Postdoctoral Program for Innovative Talents, China (Grant No. BX201700184) and the National Key Research and Development Program of China (Grant Nos. 2016YFB0400105 and 2017YFB0403102).

†Corresponding author. E-mail: xd_zhangyachao@163.com

© 2019 Chinese Physical Society and IOP Publishing Ltd

heterostructures are grown using pulsed MOCVD technique and characterized with different measurements, and the fabrication of E-mode InAlGaN/GaN metal–oxide–semiconductor HEMTs (MOS-HEMTs) with enhanced V_{TH} and output performance is demonstrated.

2. Eeperiment and results

InAlGaN/GaN heterostructures were grown on 2-inch sapphire (0 0 0 1) substrates in a vertical low pressure MOCVD system. Trimethylindium (TMIn), trimethylaluminum (TMAl), triethylgallium (TEGa), and ammonia (NH_3) were used as the precursors of In, Al, Ga, and N, respectively. The growth was initiated with a 20 nm low-temperature AlN nucleation layer and a 60 nm high-temperature AlN nucleation layer. The growth temperatures were 620 °C and 1070 °C, respectively. Then, 1.6 μm GaN buffer layer was grown at 940 °C, followed by a 2 nm AlN interlayer. Finally, the growth temperature was decreased to 700 °C for growing a 18 nm InAlGaN barrier, which was carried out by using the pulsed MOCVD technique. As shown in Fig. 1, the unit pulses of 12-s TMIn, 6-s TMAl, 6-s TEGa, and 6-s NH_3 were introduced into the reactor successively, and the metal organic pulses were always followed by the NH_3 pulses. During the pulsed MOCVD process, the growth of InAlGaN barrier was actually achieved as a series of InN/AlN/GaN short period superlattice structures. The pulsed growth method can effectively reduce the defects induced by the parasitic clathrate generated in the prereaction, and it is also beneficial to increase the adatom migration and thus improve the growth homogeneity.[20–25]

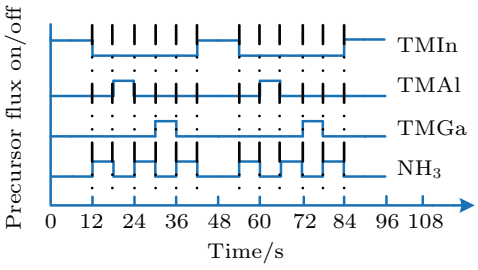


Fig. 1. Growth sequence of pulsed MOCVD for the InAlGaN barrier layer.

Several measurements were performed to investigate the material quality of the InAlGaN/GaN heterostructures. Figure 2 shows the high-resolution x-ray diffraction (HRXRD) ω–2θ scan of the InAlGaN/GaN heterostructures from the symmetric (0 0 0 6) reflection. Three dominant peaks are located at around 126.0°, 127.1°, and 137.3°, which correspond to the GaN buffer, InAlGaN barrier, and AlN nucleation layers, respectively. No additional diffraction peak can be observed, suggesting the good crystal quality of the quaternary InAlGaN materials without phase separation. In addition, the scanning electron microscope (SEM) measurement was also performed to investigate the surface morphology of the InAlGaN/GaN heterostructures. As shown in Fig. 3(a), the surface of the InAlGaN barrier is uniform and smooth, and there is no obvious macroscopic defect on it. The more detailed morphology feature was characterized by the atomic force microscopy (AFM) and the result is shown in Fig. 3(b). Clearly an atomic terrace with a few micro-pits can be observed, indicating a two-dimensional step-flow growth mode. Furthermore, the root mean square (RMS) roughness is as low as 0.29 nm in a 2 μm× 2 μm scan area. The surface morphology of the InAlGaN material in our experiment is much better than the previously reported one grown by the standard MOCVD process,[26] suggesting that pulsed MOCVD is a promising method to overcome the difficulties in the growth of high quality InAlGaN films.

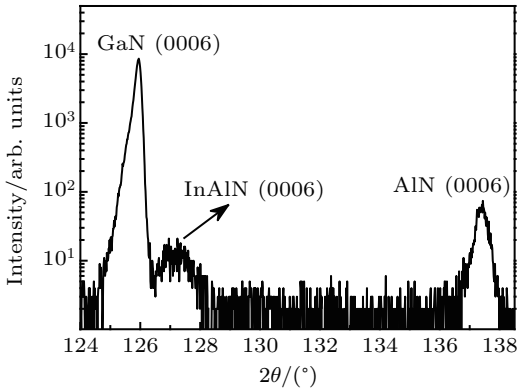


Fig. 2. HRXRD (0 0 0 6) 2θ–ω scan of the InAlGaN/GaN heterostructures grown by pulsed MOCVD.

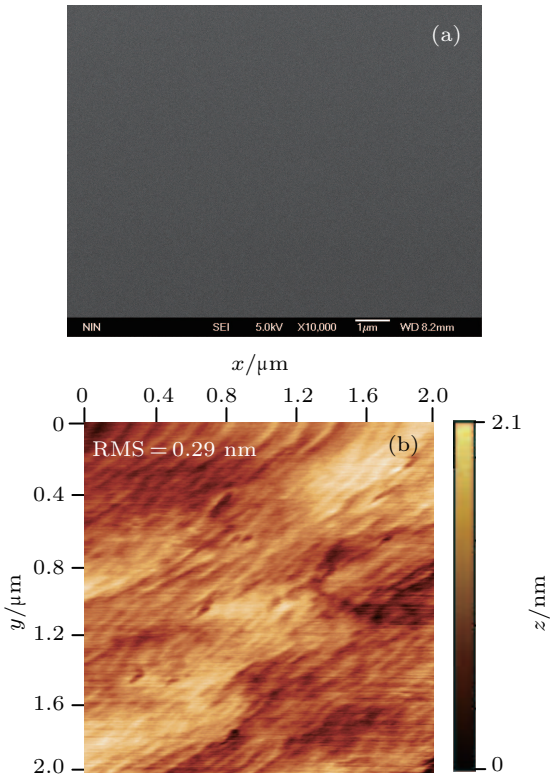


Fig. 3. (a) SEM and (b) AFM surface image of the InAlGaN/GaN heterostructures grown by pulsed MOCVD.

The precise control of the alloy composition is a key factor for the growth of InAlGaN/GaN heterostructures. Secondary ion mass spectroscopy (SIMS) was employed to accurately investigate the alloy composition of the InAlGaN barrier. Figure 4 illustrates the variation of the relative atom fractions of In, Al, and Ga with the depth from surface. It can be observed that the element content of the InAlGaN barrier layer is stable and uniform, with the In, Al, and Ga concentrations of 17%, 42%, and 41%, respectively. It can be observed that Al atoms slightly diffuse into the GaN channel layer, which may affect the transport properties of the heterostructures due to the enhanced alloy disorder scattering. This phenomenon can be suppressed by the optimization of the growth process, such as decreasing the growth rate and adding pause time between different layers. According to the previously reported results,[18] the $In_{0.17}Al_{0.42}Ga_{0.41}N$ barrier is nearly polarization matched with the GaN channel. The channel two-dimensional electron gas (2DEG) density of the $In_xAl_yGa_{(1-x-y)}N$/GaN system can be calculated based on the model proposed by Ambacher,[27,28] and the result is shown in Fig. 5. It can be observed that the 2DEG density is very sensitive to the alloy composition of the InAlGaN barrier, and the corresponding result in our experiment is 2.0×10^{12} cm^{-2}, which is much lower than that of the conventional depletion-mode heterostructures. The Hall effect measurement with the van der Pauw configuration was also carried out to further investigate the transport properties of the InAlGaN/GaN heterostructures. The 2DEG density in the channel layer is determined to be 1.8×10^{12} cm^{-2}, which shows a good agreement with the calculated result. Meanwhile, the electron mobility is as high as 1229.5 cm^2/V· s, and this result is much better than the previous ones.[13,15,17,19] Both of the calculation and experiment results indicate that the InAlGaN/GaN heterostructures achieve the nearly polarization matched condition, and the superior transport properties lay a good foundation for the E-mode MOS-HEMTs fabrication.

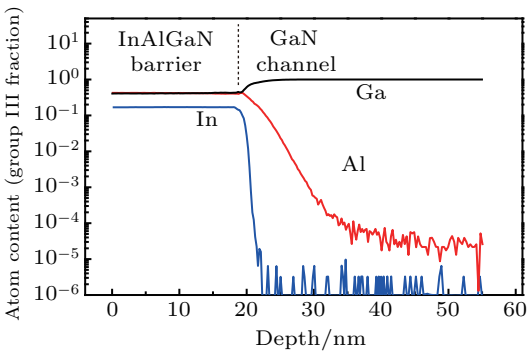


Fig. 4. SIMS depth profiles of In, Al, and Ga in the InAlGaN/GaN heterostructures grown by pulsed MOCVD.

Figure 6 shows the schematic cross-section view of the InAlGaN/GaN MOS-HEMTs, which were prepared on the as-grown nearly polarization matched heterostructures. The fabrication procedures of the MOS-HEMTs can be summarized as follows. The Ti/Al/Ni/Au (220 Å/1400 Å/550 Å/450 Å) metal stacks were firstly deposited and annealed at 85°C for 30 s to form the Ohmic contacts. Then, the mesa isolation was achieved by etching to a depth of 300 nm with the inductively coupled plasma in a Cl_2-based chemistry, followed by a 3 nm Al_2O_3 gate dielectric layer. The gate dielectric is crucial to suppress the gate leakage voltage of the E-mode devices, which usually works in the positive gate bias conditions. Finally, a gate area with length (L_G) of 1 μm was defined by the photolithograph, and a Ni/Au (450 Å/2000 Å) gate electrode was deposited. The gate-source and gate-drain distances are 1 μm and 2 μm, respectively.

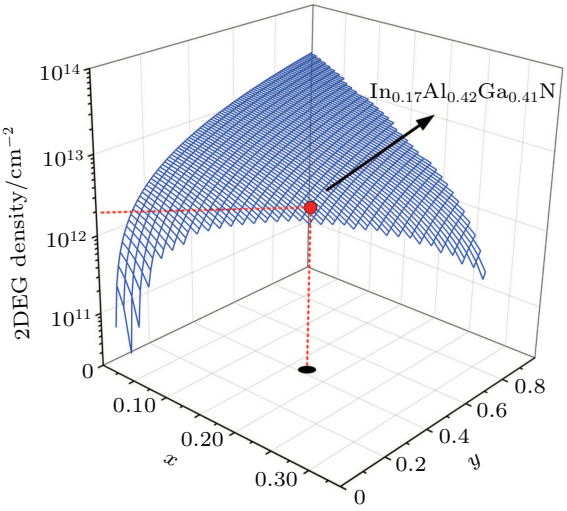


Fig. 5. Calculated 2DEG density of the $In_xAl_yGa_{(1-x-y)}N$/GaN heterostructures with different alloy composition in the barrier layer.

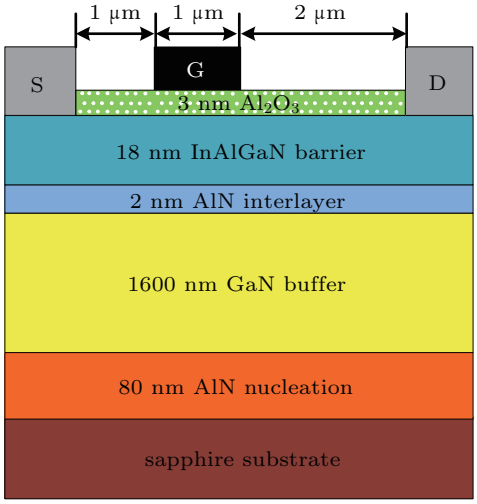


Fig. 6. Cross-section of the InAlGaN/GaN MOS-HEMTs.

The output and transfer characteristics of the MOS-HEMTs are shown in Fig. 7. The device exhibits a maximum drain current density ($I_{D,max}$) of 669 mA/mm at $V_{GS} = 6$ V

and $V_{DS} = 7$ V. The drain current I_{DS} slightly decreases with the increase of V_{DS} when $V_{DS} > 8$ V, which is related to the self-heating effects. By the method of extracting the x-axis intercept of the linear extrapolation of the I_{DS} curve at V_{GS} ($G_{m,max}$), the V_{TH} of the devices is determined to be 3.1 V. This is the first report of V_{TH} higher than 3 V for the quaternary InAlGaN based HEMTs, demonstrating their practical application value. The performance of our E-mode MOS-HEMTs is benchmarked against some state-of-the-art InAlGaN based E-mode devices in the plot of V_{TH} versus $I_{D,max}$ in Fig. 8. Our InAlGaN/GaN MOS-HEMTs grown by pulsed MOCVD possess the best V_{TH}–$I_{D,max}$ performance among the InAlGaN based E-mode devices, showing the great potential for power electronic applications. Moreover, the output characteristics available are somewhat conservative mainly resulting from the rather high Ohmic contact resistance of 1.3 Ω·mm, which results from the large bandgap of the InAlGaN barrier and the long gate length. Further improvement of device performance can be expected by optimizing the Ohmic contact and adopting advanced device processing technology like the electron beam lithography.

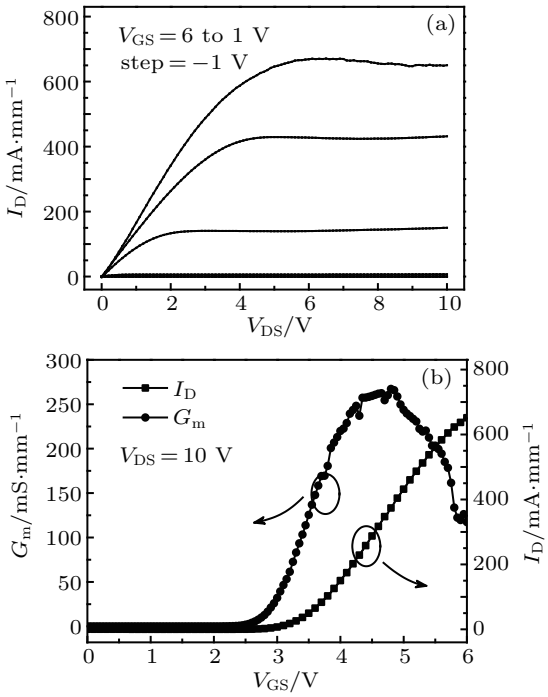


Fig. 7. (a) DC output and (b) transfer characteristics of the InAlGaN/GaN MOS-HEMTs.

In addition, the current collapse and frequency characteristics of the InAlGaN/GaN MOS-HEMTs were investigated. Figure 9(a) shows the pulsed output characteristics (using 500 ns pulses and 10 ms cycle for two quiescent points: $V_{GS} = 0$ V, $V_{DS} = 0$ V and $V_{GS} = -8$ V, $V_{DS} = 10$ V) for the InAlGaN/GaN MOS-HEMTs. It can be observed that the pulsed current is higher than the DC current, which results from the suppression of the self-heating effect. In addition, the current collapse from (0, 0) state to (−8, 10) state is related to the trapping effect.[29] The current collapse can be expressed as $(I_{(0,0)\text{state}} - I_{(-8,10)\text{state}})/I_{(0,0)\text{state}}$, which is only 6% for the InAlGaN/GaN MOS-HEMTs in our experiment. These results demonstrate the high quality of the InAlGaN material with low trap concentration, indicating the superiority of the pulsed MOCVD for growing InAlGaN quaternary alloy. As shown in Fig. 9(b), the MOS-HEMTs exhibit a current gain cutoff frequency f_t of 12.6 GHz and a unilateral power gain maximum oscillation frequency f_{max} of 23.4 GHz at a bias of $V_{DS} = 10$ V and $V_{GS} = 4.5$ V. Taking the gate length of 1 μm into consideration, this result is satisfactory and can be further improved by scaling down the device size.

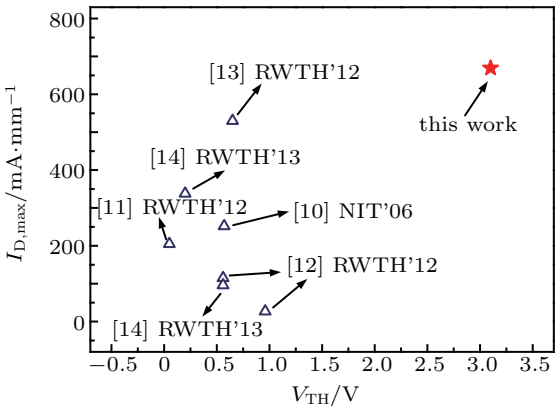


Fig. 8. The V_{TH} versus $I_{D,max}$ of some state-of-the-art InAlGaN based E-mode devices.

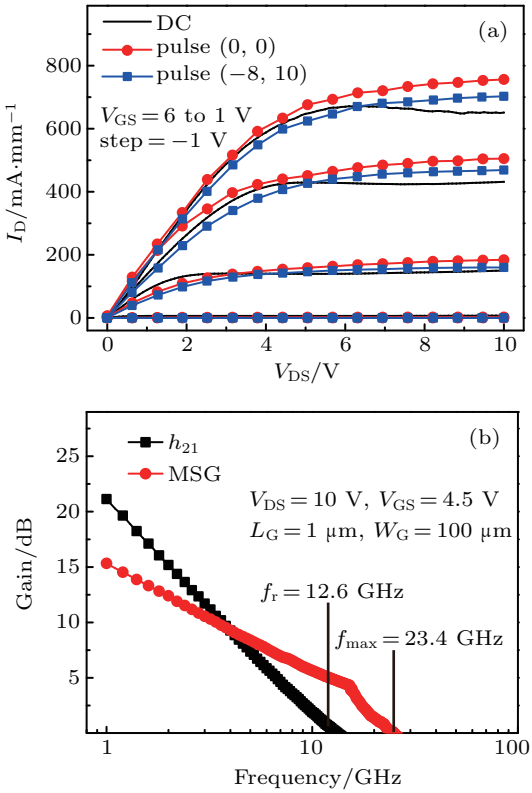


Fig. 9. (a) DC and pulsed output characteristics and (b) frequency performance of the InAlGaN/GaN MOS-HEMTs.

3. Conclusion

In summary, nearly polarization matched InAlGaN/GaN heterostructures were grown by pulsed MOCVD, and the good morphological, structural, and electrical characteristics were demonstrated in detail. In addition, high-performance E-mode MOS-HEMTs were fabricated on the prepared heterostructures, which exhibited the highest V_{TH} of 3.1 V and $I_{D,max}$ of 669 mA/mm of the InAlGaN based E-mode devices. The results strongly indicate that the InAlGaN/GaN heterostructure grown by pulsed MOCVD is a promising candidate for the fabrication of novel group-III nitride electronic devices.

References

[1] Khan M A, Bhattarai A, Kuznia J N and Olson D T 1993 *Appl. Phys. Lett.* **63** 1214

[2] Wang Y G, Feng Z H, Lv Y J, Tan X, Dun S B, Fang Y L and Cai S J 2016 *Chin. Phys. B* **25** 107106

[3] Li J, Lv Y, Li C, Ji Z, Pang Z, Xu X and Xu M 2017 *Chin. Phys. B* **26** 098504

[4] Khan M A, Chen Q, Sun C J, Yang J W, Blasingame M, Shur M S and Park H 1996 *Appl. Phys. Lett.* **68** 514

[5] Lu B, Saadat O I and Palacios T 2010 *IEEE Electron Device Lett.* **31** 990

[6] Hahn H, Lükens G, Ketteniss N, Kalisch H and Vescan A 2011 *Appl. Phys. Express* **4** 114102

[7] Cai Y, Zhou Y G, Chen K J and Lau K M 2005 *IEEE Electron Device Lett.* **26** 435

[8] Cai Y, Zhou Y G, Lau K M and Chen K J 2006 *IEEE Trans. Electron. Devices* **53** 2207

[9] Wang R, Cai Y, Tang W, Lau K M and Chen K J 2006 *EEE Electron. Device Lett.* **27** 633

[10] Deguchi T, Kikuchi T, Arai M and Yamasaki K 2012 *IEEE Electron Device Lett.* **33** 1249

[11] Mizutani T, Yamada H, Kishimoto S and Nakamura F 2013 *J. Appl. Phys.* **113** 034502

[12] Wang M, Wang Y, Zhang C, Xie B, Wen C, Wang J, Hao Y L, Wu W G, Chen K J and Shen B 2014 *IEEE Trans. Electron. Devices* **61** 2035

[13] Liu Y, Egawa T and Jiang H 2006 *Electron. Lett.* **42** 884

[14] Ketteniss N, Askar A, Reuters B, Noculak A, Hollyänder B, Kalisch H and Vescan A 2012 *Semicond. Sci. Technol.* **27** 055012

[15] Hahn H, Reuters B, Wille A, Ketteniss N, Benkhelifa F, Ambacher O, Kalisch H and Vescan A 2012 *Semicond. Sci. Technol.* **27** 055004

[16] Ketteniss N, Behmenburg H, Hahn H, Noculak A, Holländer B, Kalisch H, Heuken M and Vescan A 2012 *IEEE Electron Device Lett.* **33** 519

[17] Reuters B, Wille A, Ketteniss N, Hahn H, Hollyänder B, Heuken M, Kalisch H and Vescan A 2013 *J. Electron. Mater.* **42** 826

[18] Jena D, Simon J, Wang A, Cao Y, Goodman K, Verma J, Ganguly S, Li G, Karda K, Protasenko V, Lian C, Kosel T, Fay P and Xing H 2011 *Phys. Status Solidi A* **208** 1511

[19] Liu Y, Jiang H, Arulkumaran S, Egawa T, Zhang B and Ishikawa H 2005 *Appl. Phys. Lett.* **86** 223510

[20] Xue J, Hao Y, Zhou X, Zhang J, Yang C, Ou X, Shi L, Wang H, Yang L and Zhang J 2011 *J. Cryst. Growth* **314** 359

[21] Zhang Y, Zhou X, Xu S, Wang Z, Chen Z, Zhang J, Zhang J and Hao Y 2015 *AIP Adv.* **5** 127102

[22] Zhang Y, Zhou X, Xu S, Chen D, Wang Z, Wang X, Zhang J, Zhang J and Hao Y 2016 *Chin. Phys. B* **25** 018102

[23] Zhang Y, Zhou X, Xu S, Zhang J, Zhang J and Hao Y 2016 *Appl. Phys. Express* **9** 061003

[24] Zhang Y, Wang Z, Xu S, Chen D, Bao W, Zhang J, Zhang J and Hao Y 2017 *Appl. Phys. Lett.* **111** 222107

[25] Zhang Y, Wang Z, Xu S, Bao W, Zhang T, Huang J, Zhang J and Hao Y 2018 *Mater. Res. Bull.* **105** 368

[26] Yu S F, Chang S J, Lin R M, Lin Y H, Lu Y C, Chang S P and Chiou Y Z 2010 *J. Cryst. Growth* **312** 1920

[27] Ambacher O, Smart J, Shealy J R, Weimann N G, Chu K, Murphy M, Schaff W J, Eastman L F, Dimitrov R, Wittmer L, Stutzmann M, Rieger W and Hilsenbeck J 1999 *J. Appl. Phys.* **85** 3222

[28] Ambacher O, Majewski J, Miskys C, Link A, Hermann M, Eickhoff M, Stutzmann M, Bernardini F, Fiorentini V, Tilak V, Schaff B and Eastman L F 2002 *J. Phys. Condens. Matter.* **14** 3399

[29] He Y, Mi M, Wang C, Zheng X, Zhang M, Zhang H, Wu J, Yang L, Zhang P, Ma X and Hao Y 2017 *IEEE Electron Device Lett.* **38** 1421